The protein fold of the hyaluronate-binding proteoglycan tandem repeat domain of link protein, aggrecan and CD44 is similar to that of the C-type lectin superfamily

Nigel C. Brissett, Stephen J. Perkins*

Department of Biochemistry and Molecular Biology, Royal Free Hospital School of Medicine, Rowland Hill Street, London NW3 2PF, UK

Received 25 April 1996; revised version received 15 May 1996

Abstract Link protein and aggrecan of the extracellular matrix each contain two proteoglycan tandem repeat (PTR) domains that interact with hyaluronate. Consensus secondary structure predictions for 59 PTR sequences and 129 C-type lectin sequences give similar patterns of two α-helices and up to seven β-strands. Protein fold recognition analyses show that the 59 PTR sequences are highly compatible with the C-type lectin crystal structure. The predicted fold consists of a conserved motif formed from an antiparallel β-sheet flanked by two α-helices, the motif being attached to two distinct types of β-sheet region in the two superfamilies. Arg9 or Lys11 on an exposed loop and up to three other Arg residues in the β-sheet region are conserved and may form part of a hyaluronate binding site.

Key words: Proteoglycan tandem repeat; Hyaluronate; Link protein; Aggrecan; C-type lectin; CD44; Secondary structure prediction; Protein fold recognition

1. Introduction

Proteoglycans consist of many long anionic polysaccharide chains (glycosaminoglycans) covalently attached to an extended central protein core which stabilise the extracellular matrix [1,2]. Aggrecan is the archetypal member of this group, and contains a globular N-terminal region G1 that is constructed from an immunoglobulin fold domain and two proteoglycan tandem repeat (PTR) domains [1,2]. A second region G2 in aggrecan next to G1 contains two PTRs. Link protein also contains one immunoglobulin fold and two PTR domains [3]. G1 and link protein form a very stable ternary complex with hyaluronate. X-ray and neutron solution scattering and electron microscopy show that G1, link protein and the ternary complex possess compact structures [4–6]. Aggrecan also contains a globular C-terminal region (G3) with variable numbers of epidermal growth factor domains, followed by a carbohydrate recognition domain (CRD) belonging to group I of the C-type lectin superfamily [7], and a short consensus/complement repeat domain.

Both the PTR and CRD superfamilies are associated with carbohydrate binding, where the PTR binds hyaluronate and the CRD binds a variety of oligosaccharide ligands. The PTR superfamily includes the CD44 group of cell surface receptors. Our previous consensus secondary structure analyses of 15–20 PTR sequences indicated the occurrence of α-helices (A) and β-strands (B) in the sequence BABABBB [8]. This is very similar to our recent consensus secondary structure prediction for 129 CRD sequences which gave BABABBBB [9]. Crystal structures of rat mannose binding protein and human E-selectin in the CRD superfamily are available for comparison with these predictions [10,11].

Here, this similarity between the PTR and CRD superfamilies is examined further, using our approach to predict a protein fold prior to its crystal structure determination [12–14]. Consensus structure predictions were performed for 59 PTR sequences for comparison with our analysis of 129 CRD sequences. Protein fold recognition analyses were performed in which the 59 PTR sequences were scored against 254 known folds. These analyses showed a relationship between the PTR and CRD folds. Molecular graphics modelling of the PTR based on CRD crystal structures [10,11] showed that the PTR and CRD structures are characterised by a conserved α-helix/β-sheet core and distinct β-sheet regions. The model was examined for information relating to a hyaluronate binding site.

2. Methods

2.1. Sequence alignment and predictions

A total of 59 PTR (48 proteoglycan, 2 TSG-6 and 9 CD44) sequences were extracted from the ENTREZ CD-ROM database (National Center for Biotechnology Information) (Fig. 1). The sequence alignment followed that for 15–20 PTR sequences [4,8]. 129 CRD sequences were extracted from ENTREZ [9]. Five different methods were used to yield averaged three-state or four-state secondary structure predictions, based on the classical GOR I and GOR III and Chou-Fasman statistical methods [15–18], together with the environment-dependent amino acid substitution probability method SAPIENS [19] and the neural networking method PHD [20]. The sequence alignment was used to compute the mean hydropathy using a consensus hydrophobicity scale [15], and solvent accessibilities were computed by the SAPIENS and PHD approaches [21,22].

2.2. Protein fold recognition and modelling

All 59 PTR sequences were subjected to optimal fitting to a library of 254 protein folds using THREADER [23]. Threadings were computed in terms of pairwise interaction energies in order to evaluate the fit of each PTR sequence to a particular fold conformation. The comparison was represented as *Z*-scores [=(Energy−Mean)/Standard Deviation]. A high structural match requires a *Z*-score of less than −2.7. The *Z*-scores were sorted for input into SUM_THREADER [14] to calculate the average *Z*-score and position of each of the 254 folds from the 59 threadings.

Protein structures were visualised using INSIGHT II 95.0 (Biosym/MSI, San Diego, CA, USA) or SETOR [24] on Silicon Graphics INDY Workstations. The rigid body fragment assembly method as used in HOMOLOGY was used to model the first PTR of human link protein using the crystal structure for rat mannose-binding protein (Brookhaven code: 2msb [10]). After the definition of a 65-residue protein core, deletions were made in 2msb to define 33 loop residues in three segments in the PTR, at residues 41–47, 54–72 and 77–82. The

*Corresponding author. Fax: (44) (171) 794-9645.
E-mail: steve@rfhsm.ac.uk.

Abbreviations: PTR, proteoglycan tandem repeat; CRD, carbohydrate recognition domain of the C-lectin superfamily; G1, G2 and G3, three globular domains of aggrecan

PII S0014-5793(96)00576-5

loop conformations were constructed from a database of Brookhaven fragments. All the sidechains were mutated to those in the PTR. Energy refinements using DISCOVER were performed at the loop splice junctions, then on the loops, then on the mutated core residues. Distance constraints in these refinements were used to join Cys45 and Cys66 in the PTR. The refinements improved the connectivity of the model and reduced the proportion of bad contacts or stereochemistry, as confirmed by the use of PROCHECK [25].

The DSSP program [26] was used to assign the observed secondary structure as β-strands (DSSP codes E and B), α-helices (I, H, or G), and loop regions (s, t and .). Sidechain solvent accessibilities were calculated by the Lee and Richards method in COMPARER [27] on a scale from 0 to 9 for each residue, where 0 corresponds to 0–10% solvent exposure, 1 corresponds to 11–20% solvent exposure, and so on.

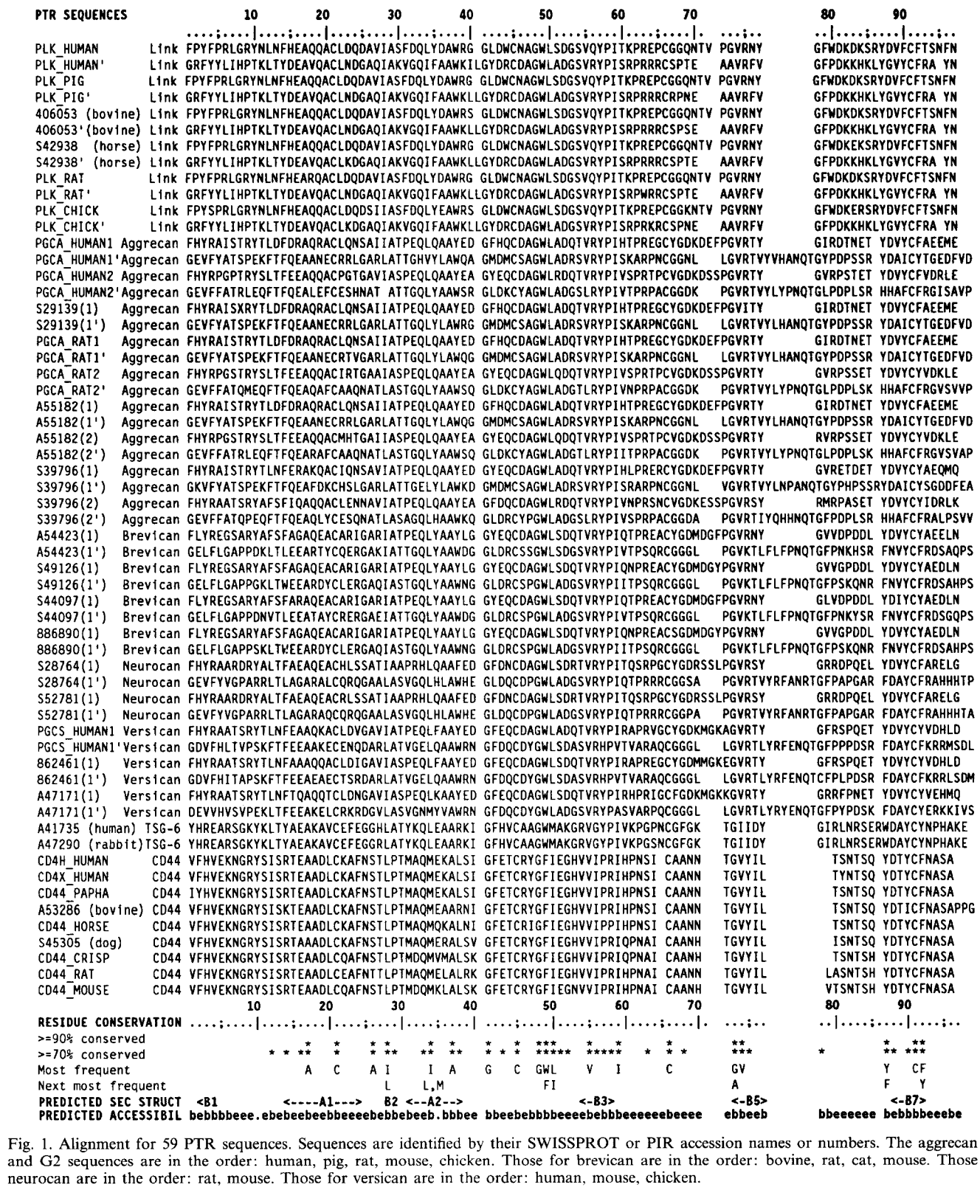

Fig. 1. Alignment for 59 PTR sequences. Sequences are identified by their SWISSPROT or PIR accession names or numbers. The aggrecan G1 and G2 sequences are in the order: human, pig, rat, mouse, chicken. Those for brevican are in the order: bovine, rat, cat, mouse. Those for neurocan are in the order: rat, mouse. Those for versican are in the order: human, mouse, chicken.

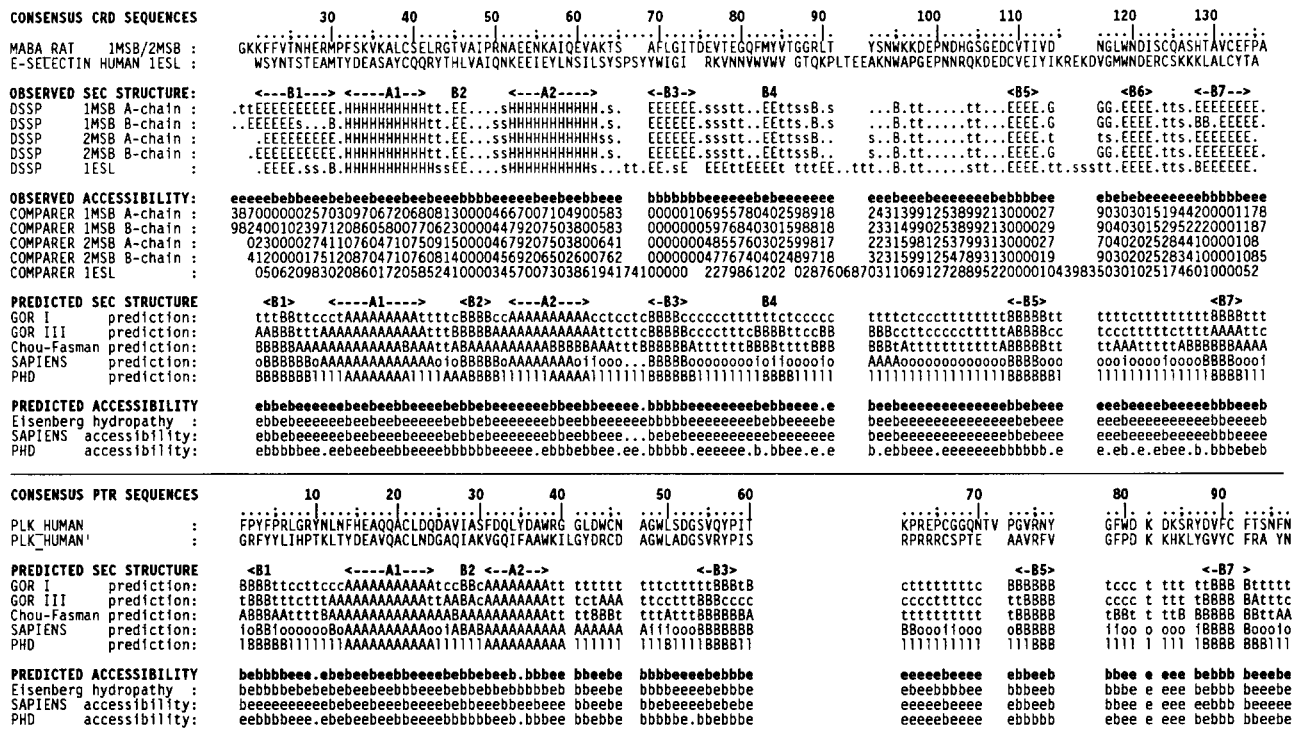

Fig. 2. Comparison of the observed and predicted secondary structures and solvent accessibilities for 5 CRD crystal structures and 129 CRD sequences with the predictions from 59 PTR sequences. Residue numberings are taken from the consensus CRD and PTR sequence alignments. The crystal structures have Brookhaven codes 1msb, 2msb and 1esl. The consensus secondary structures are indicated by arrowed regions showing α-helix (A) and β-strand (B) locations. The DSSP output is denoted by: H, α-helix; E, β-strand; other symbols are defined in Section 2. The secondary structure predictions are denoted by: A, α-helix; B, β-strand; t, turn; c, coil; l, loop; i, buried coil; o, exposed coil. The observed accessibilities have values of 0–9 (Section 2), with 0–1 corresponding to buried (b) and 2–9 to exposed (e).

3. Results

3.1. Sequence alignments and residue conservation

The alignment of 59 PTR sequences on the basis of residue similarities and minimal gap formation required only five short gaps (Fig. 1). The consensus length of the PTR was 97 residues. Both these results agree with previous analyses [5,8]. The proteoglycan subgroup (link protein, aggrecan, brevican, neurocan, versican) with 48 sequences was distinct from that of the CD44 cell surface receptor with 9 sequences. Residue conservation within the PTR superfamily was found to be high, with 19 of the 97 residues showing over 90% conservation and 37 of the 97 residues showing over 70% conservation. The highest conservation is found for the 4 Cys residues, together with 3 aromatic and 9 aliphatic residues (Fig. 1). These are presumed to form a hydrophobic core within the PTR. There are also 3 small conserved residues. These highly conserved residues occur in both the proteoglycan and CD44 subgroups except for Ala26 which is mostly replaced by Ser26 in CD44. In addition, Arg9 or Lys11 is conserved in all the PTRs except in the fourth PTR of aggrecan. Arg56, Arg63 and Arg75 are conserved in virtually all the proteoglycan subgroup, and Arg58 is conserved in the CD44 subgroup. Gln33 and Asp/Glu43 are conserved in 52 and 53 sequences respectively.

Table 1
THREADER analyses of PTR and CRD sequences

Sequences	Rank[a]	Matched fold[b]	Mean position[c]	Mean Z-score[d]
59 PTRs	1	2msb	4 ± 5	−2.5 ± 0.7
	2	1fus	12 ± 13	−1.7 ± 0.9
	3	1il1b	12 ± 24	−1.5 ± 1.7
129 CRDs	1	2msb	7 ± 22	−2.2 ± 1.3

[a]The top scoring three folds of 254 are listed.
[b]Brookhaven database codes.
[c]The mean position ± standard deviation of the 59 PTR and 129 CRD sequences in the sorted list of 254 folds after threadings.
[d]Mean pairwise interaction energy Z-score ± standard deviation for the matched fold in the 59 PTR and 129 CRD threadings.

3.2. Protein fold recognition analyses

The PTR sequences were scored for protein fold compatibility using THREADER with 254 known folds (Table 1). The use of all 59 sequences is more rigorous than the use of a single sequence [14]. The best scoring fold in terms of pairwise interaction energies was that to the CRD of rat mannose binding protein (2msb). This fold occurred 49 times out of 59 in the top five best-scoring positions of the 254 folds. The Z-scores were particularly good for many sequences, and were less than −2.7 in 23 cases and less than −3.0 in 16 cases. The mean position was 4 ± 5, and the mean pairwise interaction energy Z-score was −2.5 ± 0.7. The 2msb hit was clearly superior to others that gave close Z-scores. The next best scoring fold was 1fus (ribonuclease F1, 106 residues in an α+β fold), followed by 1il1b (interleukin 1β, 153 residues, 12 antiparallel β-strands in a six-stranded β-barrel), both of which showed noticeably greater variability in rank position and weaker Z-scores. Control THREADER calculations were performed for 129 CRD sequences [9]. As required, THREADER was able to correlate the 129 CRD sequences with its own fold (2msb) in top position (Table 1).

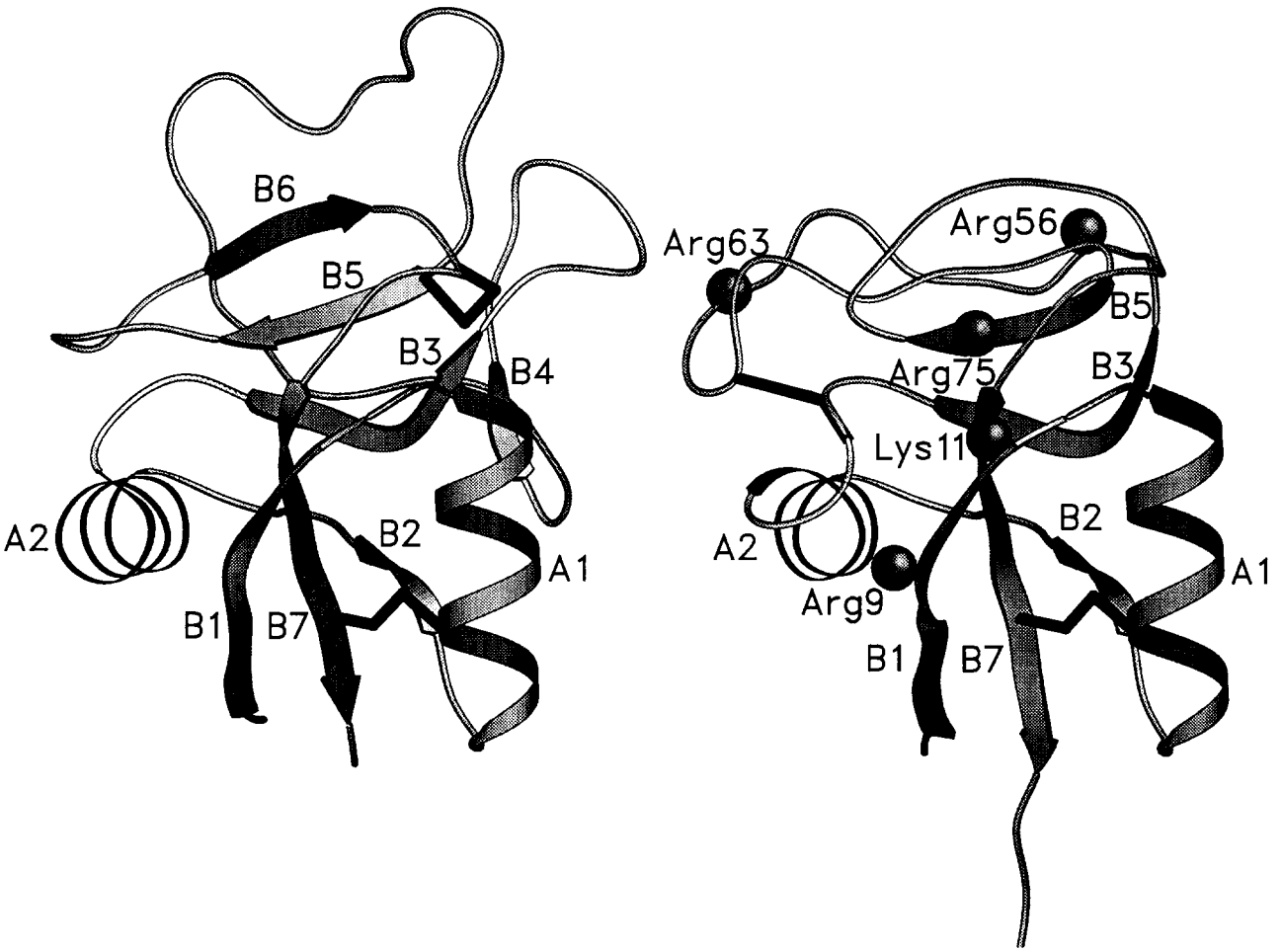

Fig. 3. Molecular graphics model of the PTR. The CRD from mannose binding protein is shown to the left in the same orientation as the PTR model to the right. α-Helices and β-strands are identified as in Figs. 1 and 2. In the PTR model, the conserved residue Arg9/Lys11 is well-defined, while the conserved residues Arg56, Arg63 and Arg75 occur in the β-sheet region which is truncated in the PTR and are less well-defined. The position of the two disulphide bridges in each fold is denoted by thick black lines.

3.3. Secondary structure and accessibility predictions

In order to correlate the CRDs with the PTRs, the averaged observed and predicted secondary structure in the CRD superfamily ([9]; manuscript in preparation) is summarised in Fig. 2. Two α-helices A1 and A2 and seven β-strands B1–B7 were consistently detected in five CRD crystal structures by DSSP analysis, although some variability in the β-strands is noticeable. Based on 129 CRD sequences, the majority votes from five predictions showed that all nine features could be detected with the exception of B6 which forms part of Ca^{2+} binding site 2 in mannose binding protein and E-selectin. In the crystal structures, the alternating e and b values for the solvent accessibilities of the α-helices A1 and A2 correspond to amphipathic structures, which was correctly predicted. The β-strands B3, B5 and B7 were observed to be buried, which was predicted correctly for B3 and B7. The β-strands B1, B2, B4 and B6 were observed to be amphipathic, and this was predicted correctly for B1, B2 and B4. These results justify the application of prediction methods to the CRD superfamily, and in turn to the PTRs.

The consensus secondary structure predictions for the PTR superfamily corresponded closely with the CRDs. The two predicted PTR α-helices A1 and A2 are close to A1 and A2 in the CRDs. Both were predicted to be amphipathic as observed in the CRDs. The two predicted PTR β-strands B1 and B2 also correlate well with the CRDs. PTR B7 correlates very well with CRD B7 as both contain a Cys residue that is bridged with one in PTR A1 [28] and CRD A1, and both B7 β-strands are hydrophobic. The PTR residues 47–85 correspond to the CRD residues 68–126, but this region is 20 residues shorter than that of the CRD. In this region, the predicted PTR β-strands B3 and B5 may be correlated with B3 and B5 in the CRDs, although B3 is now shifted in position. The PTR B6 was not predicted, but neither was it predicted in the CRD.

3.4. Molecular graphics analyses and modelling of the predicted PTR fold

The topology of the CRD 2msb fold fully accounts for the PTR prediction: (i) In the view shown in Fig. 3, the β-strands B1, B7 and B2 in the CRD form an antiparallel β-sheet at the base which is flanked by the two α-helices A1 and A2 on either side, and stabilised by a disulphide bridge. This topology accounts for the hydrophobic nature of B7 at the centre of the β-sheet. The best-predicted PTR α-helices A1 and A2 and the β-strands B1, B2 and B7 are in full agreement with this topology. This includes the conserved PTR disulphide bridge Cys21-Cys91. (ii) The antiparallel β-sheet B3-B5-B6

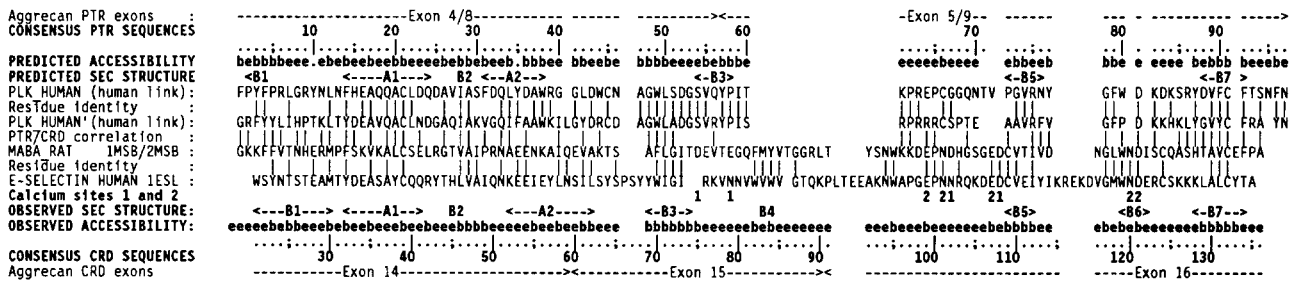

Fig. 4. Sequence alignment of the two PTRs from human link protein with the CRDs of rat mannose binding protein and E-selectin. This alignment is used for homology modelling. Residue identities between the two PTRs and two CRDs are indicated by vertical strokes. When either of the two residues in a pair of PTRs or CRDs is matched with the other pair, a vertical stroke indicates this correlation. Exon boundaries for the PTR and CRD domains in aggrecan are marked. The two Ca^{2+} binding residues in 1msb/2msb and 1esl are indicated by '1' and '2'.

form an upper region that is slightly different in the CRDs of mannose binding protein (1msb/2msb) and E-selectin (1esl). This region corresponds to the largest differences between the predicted PTR and observed CRD sequences. As 51 of the 59 residues between positions 68–126 in the CRD are in loop conformations, no firm conclusions can be inferred for the β-strands in this part of the PTR fold. It seems likely that at least B3 and B5 are present in the β-sheet region, as the topology of Fig. 3 suggests that the connection can be formed with B7 even if B6 was not present, and the innermost two β-strands B3 and B5 of the β-sheet were identified in the prediction (Fig. 2).

The predicted PTR topology was tested by the construction of a molecular graphics model. The 1msb/2msb fold was used as this gives a better alignment with the PTR from human link protein than the 1esl fold (Fig. 4). Interestingly, the 7-residue insertion between residues 77–78 in aggrecan, brevican, neurocan and versican (Fig. 1) is the same as that observed at residues 114–117 in the 1esl sequence for E-selectin. Sequence alignment of the PTR and CRD in Fig. 4 show that many residue similarities exist between B1 and B3, and again between B5 and B7, and this was used to produce a model that was stereochemically satisfactory according to PROCHECK. Energy refinement was able to generate a possible structure incorporating the required disulphide bridge between Cys45 and Cys66 on two neighbouring loops (Fig. 3). It was easier to model B6 as a loop rather than as a β-strand as Fig. 4 showed that this segment had lost two residues in the PTR sequence compared to that of the CRD. B4 in the CRD is not part of a β-sheet, and corresponds to a sequence deletion (Fig. 4) that is readily achieved in the PTR model.

4. Discussion

The inspection of our earlier secondary structure predictions for the PTRs and CRDs first raised the possibility that both superfamilies have similar folds [8,9]. This premise is supported by a combination of (i) protein fold recognition analyses; (ii) comparative predictions of secondary structures and accessibilities; (iii) sequence alignments and molecular graphics analyses. An atomic structure determination will be required to confirm the prediction. It should be noted that the prediction of a model by threading is not the same as the construction of a model by simple homology. Nonetheless the present study means that protein folds are known for all the domain types found in link protein and aggrecan [1–3], and all can be modelled.

The structural analysis of the PTR and CRD folds suggest that B1-A1-B2-A2-B7 forms a conserved α/β core framework which provides a platform for two types of β-sheet region in the PTR and CRD superfamilies. In effect, B1-A1-B2-A2 form a central slot for the insertion of the hydrophobic β-strand B7, which is then held in place by a disulphide bridge between A1 and B7 (Fig. 3). Interestingly, gene structures for aggrecan shows that B1-A1-B2-A2 are encoded by exons 4 and 8 in the first and third PTRs of aggrecan (Fig. 4), exon 4 also encodes this region in the first PTR of versican, and exon 2 likewise in the PTR of CD44 [29–32]. The CRD of aggrecan is encoded by three exons, and B1-A1-B2-A2 corresponds to the first of these, namely exon 14 [29,30]. In fact, three exons encode the group I, II and VI classes of CRDs [7].

The CRD residues that form the Ca^{2+} and carbohydrate binding sites 1 and 2 in mannose binding protein and E-selectin are found in the β-sheet region (Fig. 4). Link protein does not bind Ca^{2+}, and this concurs with the absence of these CRD residues in the PTRs. Instead Asp/Glu43 is conserved in many PTRs. Link protein is reported to possess two Zn^{2+} binding sites, of which at least one is found on the first PTR domain. Link protein also binds Ni^{2+} and Co^{2+} but not Mg^{2+} or Ca^{2+} [33,34].

The PTR model makes possible an analysis for possible hyaluronate binding sites. Basic residues in link protein have been implicated in hyaluronate binding [35,36]. Two sets of these can be considered: (i) Arg9 is conserved in the PTRs of CD44 (Fig. 1). Removal of Arg9 by site-specific mutagenesis abolished hyaluronate binding [37], and other evidence supports this role [38]. Such a hyaluronate binding site at Arg9/Lys 11 lies on an exposed surface loop (Fig. 3). Arg9/Lys11 is conserved in all the PTRs of Fig. 1 except in the second PTR of the aggrecan G2 domain when it is replaced by Gln11. As G2 in aggrecan does not bind hyaluronate [6,39,40], this is supportive of the proposed binding site. (ii) Other conserved Arg residues occur at Arg56, Arg63 and Arg75 in the β-sheet region of the proteoglycan subgroup (Figs. 1 and 3). The monoclonal antibody 8-A-4 binds to link proteins from many species and to proteoglycans [40,41]. Sequence studies show that its epitope has the sequence AGWLXDXSVXYPI [41], which includes Arg56 except when this is replaced by Gln56 in the first PTR of link protein. This epitope encompasses B3, and is located on a loop adjacent to that bearing Arg9/Lys11 (Fig. 3). The link protein peptides WDKERSRYDV/PDKKHKLYGV and QYPITKPREP/RYPISRPRKR inhibit hyaluronate binding, although this has been recently questioned [38,42,43]. The second peptide pair

correspond to Arg56 and Arg63. The involvement of Arg56 and Arg63 is compatible with the PTR model.

In summary, as discussed in [38,42], the conserved basic residues Arg9/Lys11, Arg56 and Arg63 have been implicated in hyaluronate binding in the proteoglycan subgroup of PTRs, and together with Arg75 all four are located in surface-exposed positions proximate to one another on one face of the PTR model. Two of these, Arg9/Lys11 and Arg58, are likewise conserved in the CD44 subgroup. The PTR model will be of value for future functional and structural studies of hyaluronate binding.

Acknowledgements: N.C.B. thanks the B.B.S.R.C. for a CASE studentship, and Eli Lilly for support. S.J.P. thanks the Wellcome Trust and the Royal Society for support. We are pleased to acknowledge the interest and support of Professor T.E. Hardingham and Dr T. Howe.

References

[1] Hardingham, T.E. and Fosang, A.J. (1992) FASEB J. 6, 861–870.
[2] Hardingham, T.E., Fosang, A.J. and Dudhia, J. (1992) In: Articular Cartilage and Osteoarthritis (Kuettner, K. et al., Eds.) pp. 5–20. Raven Press, New York.
[3] Neame, P.J. and Barry, F.P. (1993) Experientia, 49, 393–402.
[4] Perkins, S.J., Nealis, A.S., Dunham, D.G., Hardingham, T.E. and Muir, I.H. (1991) Biochemistry, 30, 10708–10716.
[5] Perkins, S.J., Nealis, A.S., Dunham, D.G., Hardingham, T.E. and Muir, I.H. (1992) Biochem. J. 285, 263–268.
[6] Mörgelin, M., Paulsson, M., Hardingham, T.E., Heinegård, D. and Engel, J. (1988) Biochem. J. 253, 175–185.
[7] Drickamer, K. (1993) Prog. Nucleic Acid Res. Mol. Biol. 45, 207–232.
[8] Perkins, S.J., Nealis, A.S., Dudhia, J. and Hardingham, T.E. (1989) J. Mol. Biol. 206, 737–754.
[9] Brissett, N.C. and Perkins, S.J. (1996) Biochem. Soc. Transact. 24, 99S.
[10] Weis, W.I., Drickamer, K. and Hendrickson, W.A. (1992) Nature, 360, 127–134.
[11] Graves, B.J., Crowther, R.L., Chandran, C., Rumbergewr, J.M., Li, S., Huang, K., Presky, D.H., Familletti, P.C., Wolitzky, B.A. and Burns, D.K. (1994) Nature, 367, 532–538.
[12] Edwards, Y.J.K. and Perkins, S.J. (1995) FEBS Lett. 358, 283–286.
[13] Lee, J.-O., Rieu, P., Arnaout, M.A. and Liddington, R. (1995) Cell, 80, 631–638.
[14] Edwards, Y.J.K. and Perkins, S.J. (1996) J. Mol. Biol. in press
[15] Perkins, S.J., Haris, P.I., Sim, R.B. and Chapman, D. (1988) Biochemistry 27, 4004–4012.
[16] Chou, P.Y. and Fasman, G.D. (1978) Adv. Enzymol. Relat. Areas Mol. Biol. 47, 45–148.
[17] Garnier, J., Osguthorpe, D.J. and Robson, B. (1978) J. Mol. Biol. 120, 97–120.
[18] Gibrat, J.F., Garnier, J. and Robson B. (1987) J. Mol. Biol. 198, 425–443.
[19] Wako, H. and Blundell, T.L. (1994) J. Mol. Biol. 238, 693–708.
[20] Rost, B. and Sander, C. (1993) J. Mol. Biol. 232, 584–599.
[21] Wako, H. and Blundell, T.L. (1994) J. Mol. Biol. 238, 682–692.
[22] Rost, B. and Sander, C. (1994) Proteins, 20, 216–226.
[23] Jones, D.T., Taylor, W.R. and Thornton, J.M. (1992) Nature 358, 86–89.
[24] Evans, S.V. (1993) J. Mol. Graphics, 11, 134–138.
[25] Laskowski, R.A., McArthur, M.W., Moss, D.S. and Thornton, J.M. (1993) J. Appl. Crystallogr. 26, 283–291.
[26] Kabsch, W. and Sander, C. (1983) Biopolymers, 22, 2577–2637.
[27] Sali, A. and Blundell, T.L. (1990) J. Mol. Biol. 212, 403–428.
[28] Neame, P.J., Christner, J.E. and Baker, J.R. (1986) J. Biol. Chem. 261, 3519–535.
[29] Doege, K.J., Garrison, K., Coulter, S.N. and Yamada, Y. (1994) J. Biol. Chem. 269, 29232–29240.
[30] Valhmu, W.B., Palmer, G.D., Rivers, P.A., Ebara, S., Cheng, J.-F., Fischer, S. and Ratcliffe, A. (1995) Biochem. J. 309, 535–542.
[31] Naso, M.F., Zimmermann, D.R. and Iozzo, R.V. (1994) J. Biol. Chem. 269, 32999–33008.
[32] Screaton, G.R., Bell, M.V., Jackson, D.G., Cornelis, F.B., Gerth, U. and Bell, J.I. (1992) Proc. Natl. Acad. Sci. USA 89, 12160–12164.
[33] Varelas, J.B., Kollar, J., Huynh, T.D. and Hering, T.M. (1995) Arch. Biochem. Biophys. 321, 21–30.
[34] Rosenberg, L., Choi, H.U., Tang, L.-H., Pal, S. and Johnson, T. (1991) J. Biol. Chem. 266, 7016–7024.
[35] Hardingham, T.E., Ewins, R.J.F. and Muir, H. (1976) Biochem. J. 157, 127–143.
[36] Lyon, M. (1986) Biochim. Biophys. Acta 881, 22–29.
[37] Peach, R.J., Hollenbaugh, D., Stamenkovic, I. and Aruffo, A. (1993) J. Cell. Biol. 122, 257–264.
[38] Yang, B., Yang, B.L., Savani, R.C. and Turley, E.A. (1994) EMBO J. 13, 286–296.
[39] Fosang, A.J. and Hardingham, T.E. (1989) Biochem. J. 261, 801–809.
[40] Caterson, B., Baker, J.R., Christner, J.E., Lee, Y. and Lentz, M. (1985) J. Biol. Chem. 260, 11348–11356.
[41] Neame, P.J., Périn, J.-P., Bonnet, F., Christner, J.E., Jollès, P. and Baker, J.R. (1985) J. Biol. Chem. 260, 12402–12404.
[42] Goetinck, P.F., Stirpe, N.S., Tsonis, P.A. and Carlone, D. (1987) J. Cell. Biol. 105, 2403–2408.
[43] Horita, D.A., Hajduk, P.J., Goetinck, P.F. and Lerner, L.E. (1994) J. Biol. Chem. 269, 1699–1704.